

Demonstration of a multiplexer of dissipationless superconducting quantum interference devices

J. A. B. Mates, G. C. Hilton, K. D. Irwin,^{a)} and L. R. Vale
National Institute of Standards and Technology, Boulder, Colorado 80305, USA

K. W. Lehnert
JILA, National Institute of Standards and Technology and University of Colorado, Boulder,
Colorado 80309, USA

(Received 20 July 2007; accepted 9 October 2007; published online 18 January 2008)

We report on the development of a microwave superconducting quantum interference device (SQUID) multiplexer to read out arrays of low-temperature detectors. In this frequency-division multiplexer, superconducting resonators with different frequencies couple to a common transmission line and each resonator couples to a different dissipationless SQUID. We demonstrate multiple designs, with high- Q values (4100–18 000), noise as low as $0.17\mu\Phi_0/\sqrt{\text{Hz}}$, and a naturally linear readout scheme based on flux modulation. This multiplexing approach is compatible with superconducting transition-edge sensors and magnetic calorimeters and is capable of multiplexing more than a thousand detectors in a single transmission line. © 2008 American Institute of Physics. [DOI: 10.1063/1.2803852]

Arrays of low-temperature detectors are used in many applications including astronomy,¹ nuclear and particle physics,² and materials science.³ Superconducting quantum interference devices (SQUIDs) are the amplifiers of choice for many of these detectors, including superconducting transition-edge sensors⁴ (TES) and metallic magnetic calorimeters.⁵ Since it is impractical to route wires from room temperature to each pixel in a large array at a cryogenic temperature, multiplexing techniques have developed that allow tens of SQUID-amplified detectors to be read out in each output line with bandwidth of a few megahertz.^{6,7} However, there is a need for a multiplexing technique capable of reading out thousands of detectors in a single output channel with bandwidth of a few gigahertz. Each channel must dissipate very little power on chip so that even the largest arrays do not burden the cold stage with a prohibitive heat load. Finally, for the multiplexer not to limit the sensitivity of the system, the added noise per pixel must be less than the typical output noise of a low-temperature detector.

In this paper, we demonstrate a prototype microwave SQUID multiplexer of dissipationless rf SQUIDs that meets the requirements for multiplexed readout of the next generation of low-temperature detector arrays. We demonstrate SQUIDs in resonant circuits with sufficiently high Q (4100–18 000) to provide the frequency discrimination for multiplexing hundreds or thousands of detectors. The SQUIDs have sufficiently low flux noise ($0.17\mu\Phi_0/\sqrt{\text{Hz}}$) to read out typical low-temperature detectors. This noise performance is achieved while dissipating such small amounts of parasitic power in the resonators (5 pW) that the stringent power requirements of very large arrays in space-borne observatories can be met. Finally, we demonstrate a flux-modulation scheme that linearizes the response of each pixel without requiring a separate feedback signal to each pixel.

High- Q microwave resonant circuits fabricated from superconducting coplanar waveguides provide the frequency discrimination necessary to multiplex many channels, as has been demonstrated with microwave kinetic inductance

detectors.⁸ High electron mobility transistor (HEMT) amplifiers have several gigahertz of bandwidth and dynamic range capable of amplifying the combined signals of many microwave resonators.^{9,8} However, the input noise temperature of a HEMT exceeds the output noise temperature of many low-temperature detectors; an additional stage of amplification is needed. This amplification can be provided by implementing SQUIDs between the detectors and microwave resonators¹⁰ to transduce current signals from low-temperature detectors into changes of Q ^{10,12} or of resonance frequency.^{11,13}

A dissipationless rf SQUID¹⁴ consists of a single Josephson junction interrupting a superconducting loop. Ideally, this device is a flux-variable inductor with total inductance $L_s + L_J/\cos\phi$, where L_s is the geometrical inductance of the loop, $L_J = \Phi_0/(2\pi I_c)$ is the Josephson inductance, I_c is the critical current of the junction, and $\phi/2\pi = \Phi/\Phi_0$ is the fraction of a flux quantum Φ_0 through the loop. We operate in the non-hysteretic regime, where $\lambda \equiv 2\pi\beta_L \equiv L_s/L_J < 1$ and do not shunt the junction. Because the SQUID is purely reactive, flux can be sensed without dissipating any power in the SQUID itself.

Each readout channel in the microwave SQUID multiplexer consists of a high- Q superconducting resonant circuit coupled to an rf SQUID. Current through an input coil injects magnetic flux into the SQUID loop, shifting the circuit's resonance frequency. Each channel occupies a unique frequency range of resonance frequencies, and many such resonant circuits capacitively couple to a common transmission line, known as the feedline. Each resonator modifies the amplitude and phase of microwave signals in its band that propagate along the feedline. By injecting multiple microwave tones into the feedline and monitoring the amplitude and phase of each, we may infer the current flowing in the input coil of each SQUID.

Stronger coupling between a SQUID and its resonator improves signal to noise until eventually the SQUID couples so strongly to its resonator that flux through the loop can shift the resonance by more than its width. In this state, high microwave power causes undesirable bifurcation in the resonance. We therefore target the coupling where one flux

^{a)}Electronic mail: irwin@nist.gov.

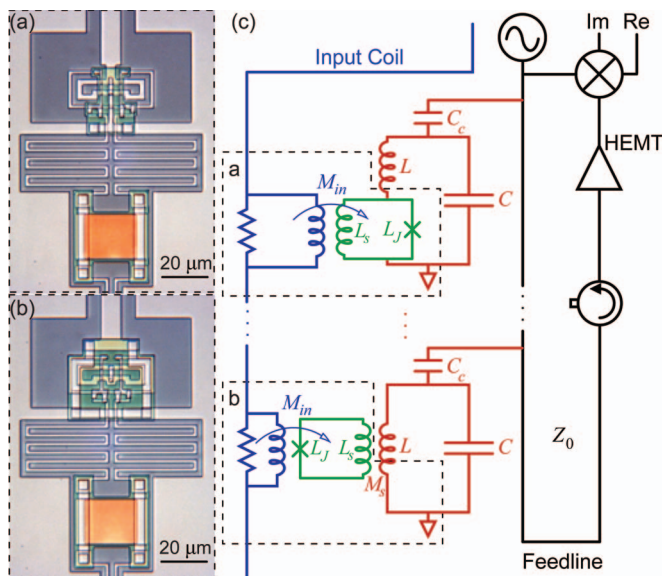


FIG. 1. (Color) SQUID photographs and circuit schematic. [(a) and (b)] Photographs of two SQUID designs. A low-pass filter takes up the bottom half of each photograph and the waveguide is just visible at the top. In (a), the SQUID is wired in series with the resonator. In (b), the SQUID inductively couples to the resonator. Both designs are gradiometric to reduce coupling to the environment. (c) Simplified schematic of the readout circuit, with the $\lambda/4$ resonators modeled as parallel LC resonators.

period of the SQUID tunes the resonance frequency, ω_0 , by the width of the resonance, ω_0/Q .

To design for this coupling, we model the resonant circuit as a flux-variable inductor $L_r(\phi)$ in parallel with a capacitance C , the combination coupled through a capacitor $C_c \ll C$ to the feedline of characteristic impedance Z_0 [Fig. 1(c)]. The resonance frequency $\omega_0 \approx 1/\sqrt{L_r C}$ is flux dependent through $L_r(\phi)$. The fractional width of the resonance is determined by the total quality factor $Q = Q_c Q_i / (Q_c + Q_i)$, where the coupled quality factor $Q_c \approx (2/\omega_0 Z_0 C_c)(C/C_c)$ describes energy loss to the feedline.

Manipulation of these equations shows that the maximum fractional shift in resonance frequency is $\Delta\omega_0/\omega_0 = \kappa^2 \lambda / (1 - \lambda^2)$, where κ^2 characterizes the SQUID-resonator coupling: $\kappa^2 = L_s/L$ if the Josephson junction couples directly to the resonant circuit in parallel with a geometrical inductance L_s as in Fig. 1(a) and $\kappa^2 = M^2/(L_s L)$ if it couples through a mutual inductance M as in Fig. 1(b). To match coupling, we thus design for $\kappa^2 \lambda Q / (1 - \lambda^2) \sim 1$. When Q is only a few thousand the directly coupled circuit can achieve the necessary large values of κ , and when Q is larger, coupling through a mutual inductance more conveniently provides smaller values of κ .

We fabricated a prototype die using our standard SQUID-fabrication process¹⁵ on bare, uncompensated Si with resistivity greater than 17 k Ω cm, etching away the SiO₂ insulating layer wherever possible to minimize dielectric noise and loss. We lithographically patterned 32 coplanar waveguide (CPW) quarter-wavelength resonators capacitively coupled to a single $Z_0 = 50 \Omega$ CPW feedline. SQUIDs are either simple or gradiometric (Fig. 1(a) and 1(b)), and resonators couple to the feedline through different coupling capacitances.

The chip was cooled in a dilution refrigerator to 17 mK inside a room-temperature mu-metal shield and cryogenic Pb shield. A signal from a microwave generator was split into

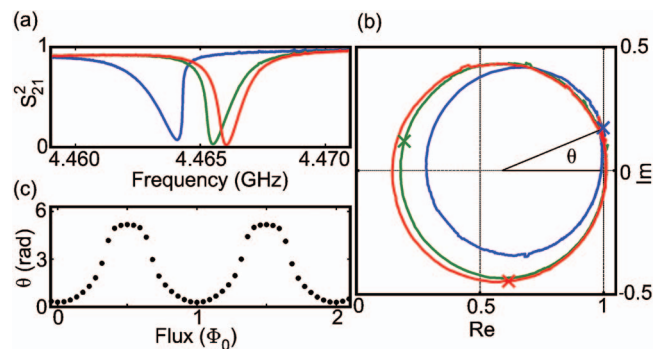


FIG. 2. (Color) Flux dependence of resonators 30 at 40 pW incident power. (a) Transmitted power as a function of frequency at three different values of flux through the SQUID, 0 (red), $\Phi_0/3$ (green), and $\Phi_0/2$ (blue). (b) Resonance circles for the same three values of flux, where 4.4654 GHz is marked (x) on each circle. (c) Angle of 4.4654-GHz on the resonance circle.

two arms (Fig. 1). One arm provided the local oscillator reference signal to a demodulator. The other arm was injected into the cryostat, attenuated, and launched along the feedline. The transmitted signal was amplified by a cryogenic HEMT amplifier with 5 K noise temperature, further amplified at room temperature, and then demodulated, extracting the components in phase (real) and 90° out of phase (imaginary) with the reference.

The resonance frequencies of the 32 resonators were approximately evenly spaced between 4.437 and 6.477 GHz. Generally, Q_c was within a factor of two of the design value, while most pixels had Q_i between 20 000 and 40 000. The effective flux noise of the SQUID designs at 100 kHz ranged between $0.17 \mu\Phi_0/\sqrt{\text{Hz}}$ and $2.23 \mu\Phi_0/\sqrt{\text{Hz}}$.

In Fig. 2, we present detailed measurements of resonator 30 [shown in Fig. 1(a)]. Resonator 30 had a measured $Q = 4100$, $Q_c = 4600$, $Q_i = 34\,000$, and $M_{in} = 5$ pH. Design parameters for this resonator were $C_c = 16$ fF, $\kappa = 0.06$, $I_c = 15 \mu\text{A}$, $L_s = 8$ pH, and $\lambda = 0.36$. Thus, $\kappa^2 \lambda Q / (1 - \lambda^2) \approx 6$, indicating that this SQUID was overcoupled. As the frequency ω of the incident microwave signal was varied close to the $\omega_0 = 4.465$ GHz resonance frequency of resonator 30, the real (in phase) and imaginary (quadrature phase) components traced out a resonance circle [Fig. 2(b)]. When the incident frequency was fixed at 4.4654 GHz, the flux in the SQUID altered the phase angle θ (measured from the approximate center of the circle) of the transmitted signal [Fig. 2(c)]. We infer the SQUID flux noise from the noise in the phase angle θ , calibrated by applying a 100 kHz, $5 \times 10^{-4} \Phi_0$ flux signal. The best flux noise was obtained by optimizing the average value of ϕ and incident microwave power $P_{inc} \approx 40$ pW. The resonance did not bifurcate at this power and the SQUID response was tolerably non-linear. We can infer the on-chip dissipation at this incident power from Q_i and Q_c to be about 5 pW. The noise power spectrum exhibits a significant $1/f$ component, but falls to $0.17 \mu\Phi_0/\sqrt{\text{Hz}}$ at 100 kHz (Fig. 3).

While fluctuations in the HEMT gain dominated the low-frequency noise in this data, additional low-frequency noise is generically seen in CPW resonators from fluctuations in the resonator dielectric.¹⁶ For the typical microwave powers in this work, the phase noise of the resonator would be smaller than the white noise level of the HEMT at frequencies around 100 kHz.¹¹ Because the signal from low-temperature detectors is typically well below 100 kHz, a flux-modulation scheme must upconvert the flux signal to

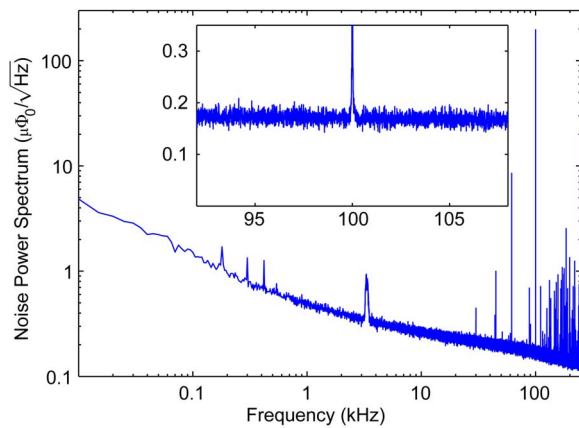


FIG. 3. (Color online) Flux noise spectrum of resonator 30. The inset magnifies the spectrum around a 100 kHz flux tone injected through the input coil to calibrate the noise.

100 kHz in order to optimize noise performance.

We implemented a flux-modulation scheme that up-converts the signal from the SQUID and linearizes the response of all pixels using a single feedback wire. In this scheme, a common flux ramp is applied to all SQUIDs. The flux ramp is a sawtooth with an amplitude of multiple flux quanta.¹¹ (A sinusoidal flux-modulation scheme has also been proposed.)¹² If the number of flux quanta per second greatly exceeds the frequency of the signal from the detector, the detector signal can be measured as a change in the phase of the periodic SQUID response. This phase change is a linear function of the detector signal and can be tracked through many flux quanta. Because this modulation technique samples the full SQUID response curve, including sections insensitive to flux, it modestly degrades the total sensitivity. For a sinusoidal response curve, the modulation degrades sensitivity by $\sqrt{2}$.

To demonstrate the flux-ramp modulation scheme, we applied both a 5 kHz, $10\Phi_0$ sawtooth signal and a lower-frequency simulated detector signal to the flux input of resonator 17 [Fig. 1(b)], which had $Q=18\,000$. For each ramp of the sawtooth we inferred the value of the simulated detector signal from the shift in the phase of the 50 kHz response (Fig. 4).

The performance exhibited by resonator 30 is sufficient to read out large arrays of TES detectors. An analysis of the resonance peaks at different flux values [Fig. 2(a)] indicates that it should be possible to space resonators less than 10 MHz apart. Thus, more than 400 pixels could be read out with one HEMT amplifier in an octave of bandwidth from 4 to 8 GHz. The measured parasitic power dissipation of 5 pW in the resonators would allow the implementation of a 100 kilopixel array with 500 nW power dissipation at the cold stage.

Finally, when we refer the excellent $0.17\mu\Phi_0/\sqrt{\text{Hz}}$ measured flux noise of the SQUID to a current noise through the relatively low input coupling of $M_{\text{in}}=5\text{ pH}$, we find that the readout adds about $100\text{ pA}/\sqrt{\text{Hz}}$. This is comparable to the noise at the output of our standard low-noise TES design.¹⁷ A modest redesign of the TES or an increase of the input-coil coupling by a factor of 3 to a still low $M_{\text{in}}=15\text{ pH}$ would

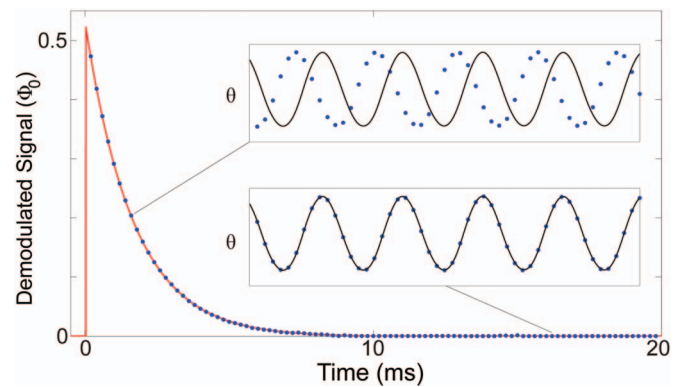


FIG. 4. (Color) (Red line) A flux signal applied to resonator 17. (Blue dots) Flux in the SQUID determined from the phase shift of the transmitted phase response, each dot corresponding to a single multiple flux quanta ramp of the modulation. The two insets show the transmitted phase θ as a function of time (expanded scale) for both a reference signal of $0\Phi_0$ (black line) and the input signal (blue dots).

ensure that the noise added by the multiplexer is below 5% of the detector noise. Significantly larger input-coil couplings will be required for optimal use with magnetic calorimeters.⁵

In conclusion, we have verified the performance of a prototype microwave-multiplexed readout of dissipationless rf SQUIDs. This technique can be used with any low-temperature detector that a SQUID can read out including TES detectors and magnetic calorimeters.

We acknowledge support from NASA under Contract No. NNH05AB771. We thank J. Zmuidzinas, S.H. Moseley, and John Clarke for useful discussions and S. Weinreb for supplying the cryogenic HEMT amplifier.

¹A. Kosowsky, *New Astron. Rev.* **47**, 939 (2003).

²R. Abusaidi, *et al.*, *Phys. Rev. Lett.* **84**, 5699 (2000).

³D. A. Wollman, S. W. Nam, G. C. Hilton, K. D. Irwin, N. F. Bergren, D. A. Rudman, J. M. Martinis, and D. E. Newbury, *J. Microsc.* **199**, 37 (2000).

⁴K. D. Irwin, *Appl. Phys. Lett.* **66**, 1998 (1995).

⁵C. Enss, A. Fleischmann, K. Horst, J. Schonefeld, J. Sollner, J. S. Adams, Y. H. Huang, Y. H. Kim, and G. M. Seidel, *J. Low Temp. Phys.* **121**, 137 (2000).

⁶J. A. Chervenak, K. D. Irwin, E. N. Grossman, J. M. Martinis, C. D. Reintsema, and M. E. Huber, *Appl. Phys. Lett.* **74**, 4043 (1999).

⁷J. Yoon, J. Clarke, J. M. Gildemeister, A. T. Lee, M. J. Myers, P. L. Richards, and J. T. Skidmore, *Appl. Phys. Lett.* **78**, 371 (2001).

⁸P. K. Day, H. G. LeDuc, B. A. Mazin, A. Vayonakis, and J. Zmuidzinas, *Nature (London)* **425**, 817 (2003).

⁹T. R. Stevenson, F. A. Pellerano, C. M. Stahle, K. Aidala, and R. J. Schoelkopf, *Appl. Phys. Lett.* **80**, 3012 (2002).

¹⁰K. D. Irwin and K. W. Lehnert, *Appl. Phys. Lett.* **85**, 2107 (2004).

¹¹K. W. Lehnert, K. D. Irwin, M. A. Castellanos-Beltran, J. A. B. Mates, and L. R. Vale, *IEEE Trans. Appl. Supercond.* **17**, 705 (2007).

¹²I. Hahn, B. Bumble, H. G. LeDuc, M. Wilert, and P. K. Day, *Ann. Isr. Phys. Soc.* **850**, 1613 (2006).

¹³K. D. Osborn, J. A. Strong, A. J. Sirois, and R. W. Simmonds, e-print arXiv:cond-mat/0703103.

¹⁴K. K. Likharev, *Dynamics of Josephson Junctions and Circuits* (Gordon and Breach, Amsterdam, 1996).

¹⁵J. E. Sauvageau, C. J. Burroughs, P. A. A. Booij, M. W. Cromar, S. P. Benz, and J. A. Koch, *IEEE Trans. Appl. Supercond.* **5**, 2303 (1995).

¹⁶J. Gao, J. Zmuidzinas, B. A. Mazin, H. G. LeDuc, and P. K. Day, *Appl. Phys. Lett.* **90**, 102507 (2007).

¹⁷J. N. Ullom, J. A. Beall, W. B. Doriese, W. D. Duncan, L. Ferreira, G. C. Hilton, K. D. Irwin, C. D. Reintsema, and L. R. Vale, *Appl. Phys. Lett.* **87**, 194103 (2005).